Energy & Environmental Science

Accepted Manuscript

ROYAL SOCIETY OF CHEMISTRY

www.rsc.org/ees

Energy & Environmental Science

RSCPublishing

COMMUNICATION

Efficient and selective carbon dioxide reduction on low cost protected Cu_2O photocathodes using a molecular catalyst

Marcel Schreier, Peng Gao, Matthew T. Mayer, Jingshan Luo, Thomas Moehl, Mohammad K. Nazeeruddin, S. David Tilley and Michael Grätzel*

Cite this: DOI: 10.1039/x0xx00000x

Received 00th October 2014,
Accepted 00th October 2014

DOI: 10.1039/x0xx00000x

www.rsc.org/

Photoelectrochemical reduction of CO_2 to CO was driven by a TiO_2-protected Cu_2O photocathode paired with a rhenium bipyridyl catalyst. Efficient and selective CO evolution was shown to be stable over several hours. The use of protic solution additives to overcome severe semiconductor-to-catalyst charge transfer limitations provided evidence of a modified catalytic pathway.

Introduction

Since the beginning of industrialization, atmospheric carbon dioxide (CO_2) levels have been on the rise. Being a greenhouse gas, the high levels of CO_2 are a major contributor toward global warming.[1] Several strategies for reducing global CO_2 concentrations are being investigated, ranging from decreasing the anthropogenic output to capturing CO_2 from the atmosphere and storing it underground.[2,3] However, the ultimate way of controlling atmospheric CO_2 levels is to close the anthropogenic carbon cycle by using CO_2 as a feedstock for fuel production from renewable energy sources.

Transforming CO_2 is an endergonic process, and accomplishing it on a global scale will require large amounts of energy. Driving the conversion of CO_2 with sunlight, the primary source of renewable energy,[4] allows for the storage of solar energy in the form of carbon-based fuels. This can be achieved by, for instance, a photoelectrode functionalized with a suitable catalyst to drive a reaction of interest.[5–8] Our group has made substantial progress on the use of metal oxides as photoelectrodes, materials advantageous for their earth-abundance and low-temperature synthetic methods, leading to cheap and easy to produce devices.[9,10] A notable advance was the stabilization of p-type cuprous oxide (Cu_2O), inherently unstable under reductive conditions, by employing an amorphous TiO_2 overlayer.[10–13] Follow-up work on this surface protection approach has shown it to be broadly compatible with a variety of photoelectrode materials, leading to significantly enhanced stabilities of materials previously known to be unstable in solution under operation conditions.[14–20]

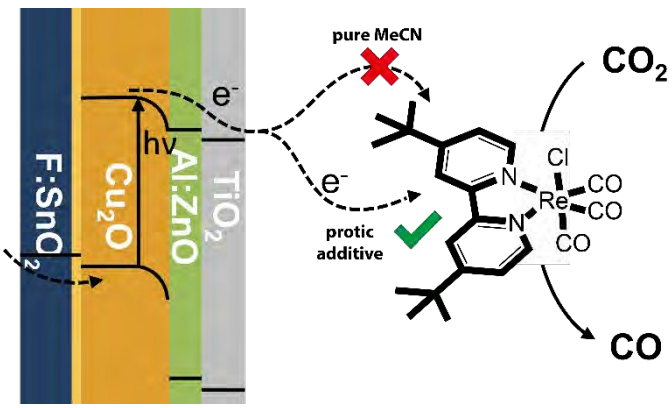

Fig. 1: Schematic of the photoelectrochemical CO_2 reduction process involving protected Cu_2O photocathodes and a Re-based molecular catalyst.

Despite their success, protected photocathodes, most notably the protected Cu_2O, have only been applied towards the reduction of water to produce hydrogen gas. Approaches toward the photoelectrochemical reduction of CO_2, meanwhile, have been mostly limited to expensive III-V compounds and crystalline silicon photocathodes, and only a few reports have studied the interaction between photoelectrodes and molecular

catalysts.[8,21–24] In this work we investigated the photoelectrochemical reduction of CO_2 using TiO_2-protected Cu_2O in an effort to demonstrate a low-cost approach to CO_2 reduction while broadening the fuels products accessible from these electrodes. Our research led to the discovery of unique charge transfer effects from semiconductor surfaces and to a new way of tuning charge transfer at these interfaces through changing the catalytic pathway.

In the first demonstration (to the best of our knowledge)[8] of driving a molecular CO_2 reduction catalyst with a metal oxide photoelectrode, we paired the catalyst Re(tBu-bipy)$(CO)_3$Cl, introduced by Kubiak *et al.*,[25] with a TiO_2-protected Cu_2O photocathode in CO_2-saturated acetonitrile as illustrated schematically in Fig. 1. Illuminating with simulated sunlight led to cathodic photocurrent densities exceeding 2 mA cm^{-2}, the highest currents for CO_2 reduction on an all-oxide photocathode. A sustained current density of 1.5 mA cm^{-2} was achieved when biased at a potential where previous photocathode attempts gave negligible catalytic currents,[21] a result of the use of a protic additive combined with the 560 mV photovoltage provided by the Cu_2O photocathode. We confirmed that the photocurrent corresponded to selective CO evolution with 100% faradaic efficiency, and was stable over several hours. Interestingly, we observed a critical charge transfer limitation from the TiO_2 surface to the catalyst which was not seen when using a glassy carbon electrode, signifying a fundamental difference between semiconductor and metal-like electrodes for this molecular system. A key discovery was that the simple addition of a protic additive such as methanol or n-propanol could remove this limitation to yield the full light intensity-limited photocurrent. We propose that the additives act to modify the charge state of the catalyst intermediate to avoid electrostatic repulsion between molecule and semiconductor, a new and important finding for the future use of semiconductors toward this process which simultaneously provides insight into mechanistic details of the catalytic process. Furthermore, we show that the TiO_2 protection layer is necessary to achieve stable currents and selective CO generation, as bare Cu_2O photocathodes degrade quickly and yield H_2 as the dominant reaction product. This signifies that the TiO_2 protection strategy is robust and versatile, and signals that the understanding of the charge transfer from this surface can lead to widespread use of various protected photoelectrodes toward CO_2 reduction by molecular catalysts.

Results and discussion

Performance under chopped light

The photocathodes used in this study were prepared as previously reported, wherein a crystalline cuprous oxide film (500 nm), grown by electrodeposition onto a conductive fluorine-doped tin oxide (F:SnO_2, FTO) substrate, is covered by sequential atomic layer deposited (ALD) films of aluminium-doped zinc oxide (Al:ZnO; 20 nm) and titanium oxide (TiO_2; 100 nm), resulting in the conformal heterojunction device depicted by cross-section micrograph in Fig. S1 (complete experimental details are provided in the Supplementary Information). Fabrication of the device uses exclusively earth-abundant materials and is carried out at temperatures below 150 °C, while ALD uses only moderate vacuum. This leads to a low cost and easy to produce photoelectrode which is readily scalable, representing the main advantages of this material.

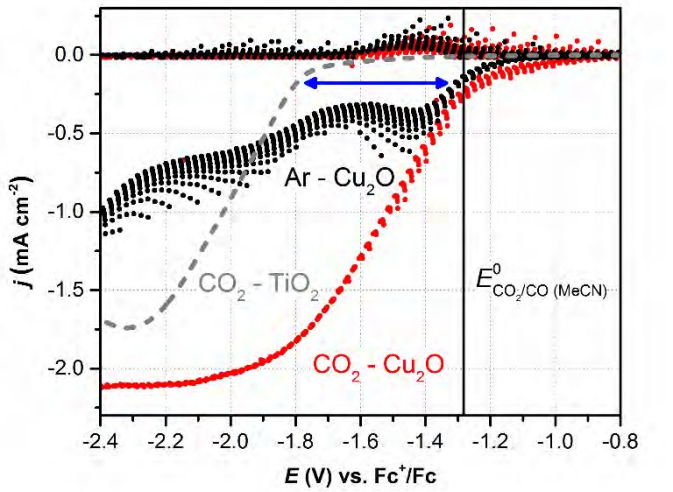

Fig. 2: Chopped light linear sweep voltammetry of the Cu_2O photoelectrode with 2 mM Re(tBu-bipy)$(CO)_3$Cl in the presence of 1.0 M MeOH under argon (black curve) or under CO_2 (red curve), compared to the same linear sweep at an FTO-TiO_2 electrode under CO_2 in the dark (grey curve). The arrow indicates the observed photovoltage of 560 mV, and the vertical line labels the reversible potential of the CO_2/CO couple in MeCN.[26]

To examine the CO_2 reduction activity of this device, photoelectrochemical experiments were carried out using simulated solar light (AM 1.5G) in anhydrous acetonitrile solution containing 0.1 M of Bu_4NPF_6. The solutions contained 2 mM of Re(tBu-bipy)$(CO)_3$Cl as catalyst and were saturated with either argon or carbon dioxide. When using a solution containing 1.0 M methanol (MeOH) as a protic additive, chopped illumination experiments revealed a strong cathodic photocurrent response when under CO_2 saturation, as compared to a weaker and unsustained photocurrent response when saturated with argon, clearly demonstrating the current flow towards reducing carbon dioxide (Fig. 2).

Compared to an amorphous TiO_2 surface in the dark, which is analogous to the surface of the photocathode, a photovoltage shift of 560 mV combined with a good fill factor was observed. A similar photovoltage is found when compared against a glassy carbon electrode (discussed later), consistent with the photovoltage observed from similar photocathodes in water splitting applications.[11] Additionally, we observe a photocurrent density of 2.1 mA cm^{-2}, which to our knowledge is the largest current density obtained towards CO_2 reduction on an oxide material. In this system, through the photovoltaic activity of the photocathode, we were able to observe an onset of reductive photocurrent which is positive of the -1.28 V vs. Fc^+/Fc reversible potential of carbon dioxide reduction in acetonitrile.[26] Additionally, through the use of MeOH as an electrolyte additive, we obtained a significantly earlier onset than shown in

previous studies using silicon as photocathodes,[21,22] leading to sustained CO_2 reduction at potentials where those devices do not yet produce a catalytic onset.

Over the entire potential range tested, only negligible dark currents were observed, thereby pointing towards the excellent performance and stability of the photocathode device, even at potentials significantly more negative than those used in water reduction demonstrations. This is notable since unprotected cuprous oxide devices degrade severely under these conditions (see below).

The currents observed in the absence of CO_2 (under argon saturation) correspond to reduction of the catalyst itself but without leading to a catalytic turnover. This is supported by the presence of current transients upon light chopping under argon, transients which originate from the transport-limited diffusion of catalyst molecules toward the electrode surface. Current transients are no longer observed in the presence of CO_2 since as soon as a catalyst molecule has been reduced, it catalyzes the reduction of CO_2 and returns to its oxidized state, allowing its rapid re-reduction by the photocathode and thereby supporting sustained currents.

Light intensity response

The absence of transients in the presence of carbon dioxide (Fig. 2) suggests that diffusive transport no longer limits the photocurrent, but rather that the incident light intensity becomes the limiting factor. To verify this hypothesis, linear sweep scans were carried out under various intensities of simulated sunlight. As seen in Fig. 3, and in its inset showing the plateau photocurrent as a function of light intensity, in the presence of 1.0 M MeOH as additive it was indeed found that the measured photocurrent varied linearly with the incident light intensity, thus supporting that the photocurrent is now limited by the photon flux arriving at the photoelectrode. It should be noted that due to the design of the photoelectrochemical cell, the light must travel through 1 cm of strongly yellow colored catalyst solution which absorbs a non-negligible part of the solar light, thus explaining the observation of lower photocurrents relative to those achieved in water splitting applications. Indeed, increasing the catalyst concentration above 2 mM led to a decrease in photocurrents, as shown in Fig. S2. Optimization of the cell design is therefore a path toward enhancing the photocurrents.

Surprisingly, a proportionality between the photocurrent and incident light intensity was not observed in the absence of a protic additive. Without MeOH, the observed photocurrent saturated for light intensities beyond 14%, whereas the quasi Fermi level of the electrons continued to rise with increasing light intensity, as indicated by a progressively more positive reduction onset (see Fig. S3 for a detailed plot). Although the first catalyst reduction takes place similarly in the absence and presence of a protic additive, further reductions seem to be severely hindered. This points to a critical interfacial charge transfer limitation which is not related to the photovoltaic efficiency of the photoelectrode. This effect and its implications will be discussed in more detail below.

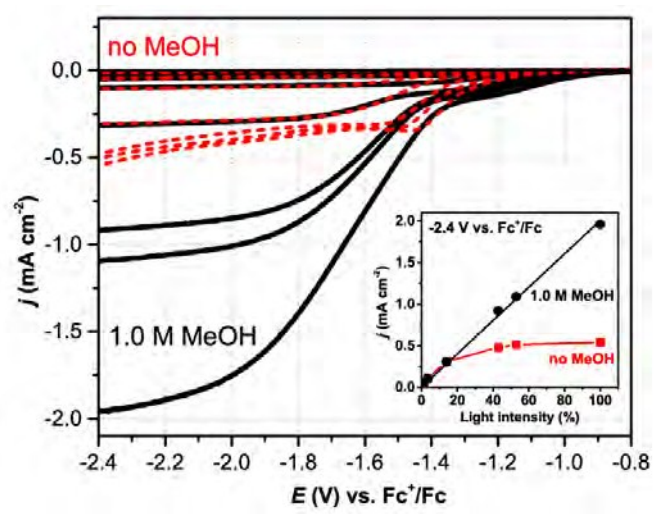

Fig. 3: Linear sweep scans of the Cu_2O photoelectrode with 2 mM Re(tBu-bipy)$(CO)_3Cl$ under CO_2 (50 mV sec^{-1}) in the absence (red) and presence (black) of 1.0 M MeOH, under 0, 1.2, 3.5, 14, 43, 53 and 100% simulated AM 1.5 illumination (top to bottom line). In the absence of MeOH, despite the increased photon flux and consequently increased quasi Fermi level of the electrons, no increase of catalytic current is visible above 14%. In the presence of MeOH, the photocurrent scales linearly with the light intensity as can be seen in the inset, showing the observed current density at -2.4 V vs. Fc+/Fc at the various incident light intensities.

Sustained current stability test

From these investigations we identified protic additives as a strategy to facilitate efficient turnover of carbon dioxide on the protected cuprous oxide photocathode. Under these conditions, the quantitative production of carbon monoxide was investigated at -1.73 V vs. Fc^+/Fc, a potential which is near the onset of the first catalyst reduction on a glassy carbon electrode. The current density and faradaic efficiency over several hours under CO_2 saturation and periodically chopped illumination are shown in Fig. 4. The inset details the absence of dark current, and the small perturbations of the photocurrent can be attributed to accumulated carbon monoxide bubbles releasing from the electrode surface. The generation of CO bubbles is shown in Fig. S4 and in the movie as supporting information. During stability tests, interrupting the light source for 2 seconds following each 2 minute period allowed us to verify the continued photoactivity of the device. This is important since it confirms the generation of true photocurrent, rather than corrosion processes which would manifest as an increase in the dark current. The negligible dark current even after 5 hours of testing shows the effectiveness of the protective TiO_2 overlayer and overall stability of the device.

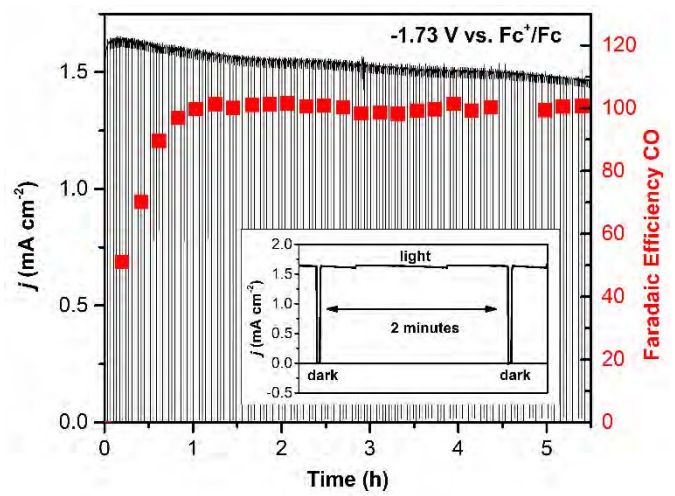

Fig. 4: Cathodic current density and CO evolution efficiency of the Cu_2O photocathode under chopped light at a constant potential of -1.73 V vs. Fc^+/Fc with 2 mM $Re(tBu\text{-}bipy)(CO)_3Cl$ and 7.5 M MeOH under CO_2. Both current density (black line) and faradaic efficiency towards carbon monoxide (red dots) are reported. The initial increase in CO efficiency is attributed to the gradual saturation of the electrolyte. The inset shows a zoomed view of the recorded current, showing the absence of dark current and the occasional changes in current density due to CO gas bubbles detaching from the electrode surface. Only little performance loss is observed over 5.5 hrs and can be mainly attributed to increased light absorption by the catalyst due to evaporation of the solvent.

For the duration of the test, CO_2 flowed through the headspace of the photoelectrochemical test cell and the product gas was analyzed on-line by gas chromatography. From the gas measurements, a strong CO signal developed whereas only trace amounts of hydrogen were observed (Fig. S5), confirming that the observed bubbles corresponded to carbon monoxide generation. When related to calibration with a CO standard, a quantitative current yield towards the production of carbon monoxide was confirmed, within experimental error. Over 5.5 hours, a small decrease of photocurrent was observed, attributable to solvent evaporation and the concomitant increase in the catalyst concentration and its light absorption (shown above to be the current-limiting factor). To the best of our knowledge, this represents the longest stability shown for an oxide-based system towards CO_2 reduction. The good performance and quantitative CO yield of our system is notable since we are operating at a potential where previous reports using silicon as photocathodes did not even observe the onset of catalytic currents. The earlier onset results from the combination of the device photovoltage as well as a changed catalyst mechanism in the presence of MeOH, discussed in more detail in the final section.

The importance of protective layers

A possible simplification of the device is the use of unprotected Cu_2O as a p-type semiconductor in direct contact with the electrolyte, a configuration which should theoretically be capable of producing cathodic photocurrents in this system. Long-term polarization tests were carried out using this material under conditions identical to the stability test described previously. It was found that within a few minutes, the photoactivity was lost whereas significant dark currents remained, and the gas analysis showed the production of large amounts of hydrogen but only trace CO (Fig. S5), thereby indicating the degraded Cu_2O photocathode acts as a catalyst for hydrogen evolution from non-aqueous acids. Scanning electron microscopy analysis of the bare and protected Cu_2O electrodes before and after the polarization tests showed the emergence of a particulate morphology on the unprotected surface while the morphology of protected Cu_2O photocathodes remained unchanged after several hours of polarization (Fig. 5). To examine compositional changes in these devices, x-ray diffraction analysis was performed (Fig. S6), revealing that while the protected electrodes experienced no observable changes in diffraction pattern, the unprotected Cu_2O clearly showed the emergence of metallic copper due to corrosion under reaction conditions. It is therefore apparent that TiO_2 protection layers are important for sustained CO_2 reduction to be possible on a Cu_2O photocathode, even in the absence of water.

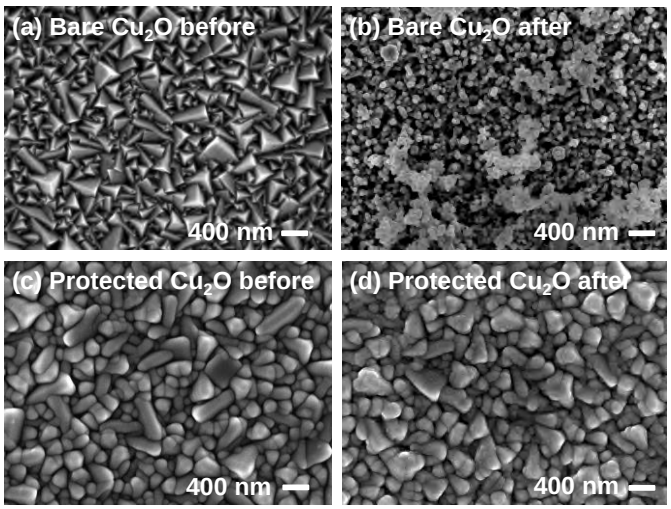

Fig. 5: SEM micrographs of unprotected Cu_2O before (a) and after (b) polarization at -1.73 V under AM 1.5G illumination in presence of 2 mM of catalyst and 7.5 M MeOH. Significant corrosion of the photocathode becomes obvious. In contrast, SEM micrographs of TiO_2-protected Cu_2O before (c) and after (d) polarization show no morphological changes, indicating that the material is stable under reaction conditions.

The role of protic additives

One of the most striking observations of the data presented above is that in the absence of MeOH, charge transfer from the photocathode to the molecular catalyst was severely limited and no catalytic onset was observed. This was in contrast to a glassy carbon electrode where, in agreement with the literature, the second reduction of the catalyst happened concomitantly with the onset of catalytic current (Fig. 6a, black; similar behavior was observed on Au and Pt, not shown).[25] Adding protic solvents allowed us to overcome the observed limitations on the photocathode, which constitutes a new and intriguing finding which warrants further discussion.

The above tests at different light intensities (Fig. 3) suggested that the limitations in current density on Cu_2O photocathodes are

due to an interfacial charge transfer effect, rather than due to the internal photovoltaic activity of the photocathode. Since the interface of the photocathode is defined by the TiO_2 protection layer, the interaction between TiO_2 and the molecular catalyst was suspected to be the culprit in hindering charge transfer.

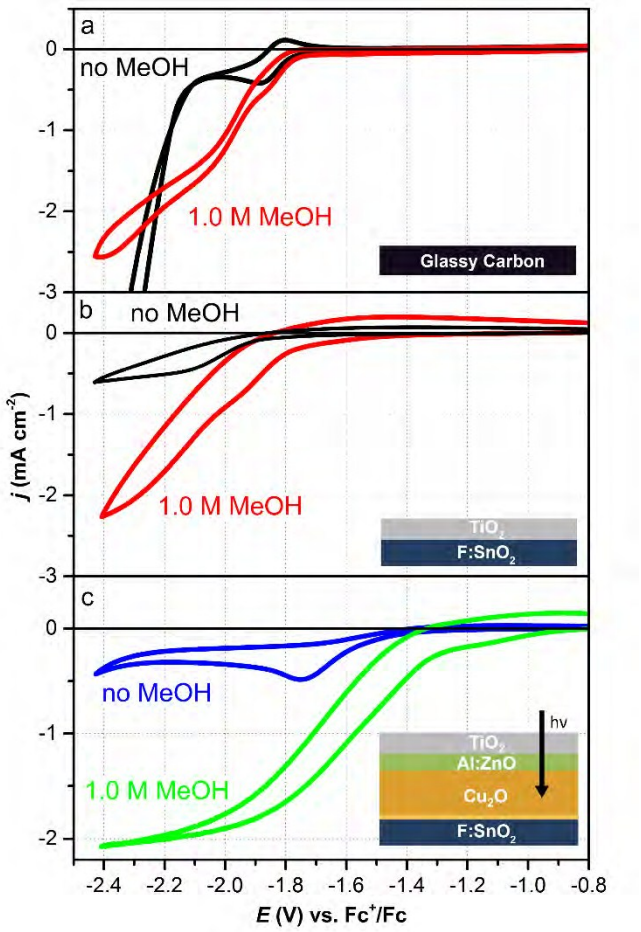

Fig. 6: CV scans of 2mM Re(tBu-bipy)$(CO)_3Cl$ under CO_2, in absence and presence of MeOH at (a) glassy carbon in dark, (b) ALD TiO_2 on FTO in dark, and (c) on the protected photocathode under simulated AM 1.5 illumination. Scan rate 100 mV/sec. The absence of a catalytic current on the TiO_2 surface in the dark as well as on the TiO_2-terminated photocathode is striking. The limitations can be overcome by adding a protic solvent such as MeOH to the electrolyte.

This hypothesis was confirmed by carrying out cyclic voltammetry (CV) experiments on ALD TiO_2 deposited on bare FTO substrates, thereby acting as dark electrodes with surfaces similar to the photocathodes. In CO_2-saturated catalyst solutions (Fig. 6b, black; detailed in Fig. S8), these electrodes showed similar charge transfer limitations as the photocathode (Fig. 6c, blue), confirming that its TiO_2 surface is the element hindering charge transfer in the absence of a protic additive. In addition, just as observed on the photocathode, protic additives such as MeOH and n-propanol (Fig. S10) led to a significant enhancement of electron transfer from the TiO_2 surface, and, most notably, to greater similarity between CVs on TiO_2 and on glassy carbon (Fig. 6a and b, red). A comparable behavior was also observed on crystalline anatase TiO_2 electrodes (Fig. S9).

We hypothesize that the cause of this effect is found in a changed catalytic pathway at the molecular level. On glassy carbon, the presence of a protic additive clearly led to a significantly changed mechanism as evidenced by the CV plots of Fig. 6a, with the complete loss of reversibility of the first reduction wave pointing to a rapid conversion of the catalyst once it has been reduced. This was accompanied by an earlier onset of catalytic current (see Fig. S11 for the CO_2-free comparison) and a different turnover mechanism when compared to the CV in the absence of a protic additive.

Compelling evidence for the change in catalytic pathway is found in comparison of the CV responses on semiconductor (TiO_2) and metal-like (glassy carbon) electrodes. Consider that the single electron reduction of the catalyst to Re(tBu-bipy)$(CO)_3Cl^-$ (without loss of the chloride ligand) will produce a charged (anionic) catalyst intermediate.[27,28] This species should interact differently with metal and semiconductor electrodes due to differences in surface charge. On an n-type TiO_2 electrode, cathodic current flow requires the semiconductor to go into accumulation, resulting in a buildup of localized electrons through the filling of trap and conduction band states close to the electrode surface (see Fig. S7 for illustration).[29,30] This will produce a significant surface charging effect, in contrast to metal-like electrodes which generally exhibit shorter Debye lengths due to more effective charge screening.[31]

The difference in charging between electrode types is the proposed cause of the disparities observed in the methanol-free CVs of Fig. 6. Formation of the anionic intermediate Re(tBu-bipy)$(CO)_3Cl^-$ in the first reduction leads to coulombic repulsion of this species from the negatively charged semiconductor surface, thereby inhibiting a second reduction from taking place. Meanwhile, the absence of coulombic repulsion on the metal-like glassy carbon surface allows the second reduction and catalyst turnover to occur readily, albeit at a more negative potential.

In contrast, a catalyst pathway avoiding a charged intermediate should allow the second reduction to occur even on a charged semiconductor surface. We propose that in the presence of protic additives like methanol, abstraction of the chloride ligand from the catalyst (previously shown to be a crucial step in catalyst activation) is significantly enhanced, likely through hydrogen bonding of the protic species to chloride,[32] leading to an enhancement of chloride dissociation. This is in agreement with what has recently been proposed for a similar catalyst in ionic liquid solvent.[27] If chloride abstraction is enhanced, a neutral intermediate Re(tBu-bipy)$(CO)_3$ would form upon first reduction, which now in absence of coulombic repulsion will promptly be reduced again even at a charged semiconductor electrode, enabling the turnover of the catalyst to take place on TiO_2 as we observed in Fig. 6. Improved abstraction of Cl^- therefore has significant implications on the catalytic activity of this class of CO_2 reduction catalysts on semiconductor surfaces.

It is believed that the catalytically active form of this Re(bipy) class of molecules is the doubly-reduced and chloride free Re(bipy)$(CO)_3^-$ product.[33] Nevertheless there remains some uncertainty in the literature regarding the sequence of chloride

ligand loss, whether it occurs before or after the second reduction.[25,27,28,34] Several reports have suggested that the catalyst activation happens upon loss of Cl^- following the second reduction of the molecule.[27,28] The fact that in our data the addition of MeOH gave a pronounced change in the CV on glassy carbon, namely the loss of reversibility of the first reduction and the absence of a CV crossover (Fig. 6a), suggests a significant mechanistic change. Furthermore, enabling of unimpeded charge transfer on TiO_2 and on TiO_2-protected photocathode electrodes (Fig. 6b,c) points to a change in charge state of the catalyst intermediate, as explained above. We therefore propose that in the presence of a protic species the catalytic pathway is modified to one in which the chloride abstraction precedes further catalyst reduction, resulting in a neutral intermediate that avoids coulombic repulsion limitations to charge transfer. This is a distinct claim that is under further investigation in our lab; however, multiple reports support the pathway of chloride loss before second reduction.[25,34]

We note that effects similar to those observed here may help explain the charge transfer limitation reported on p-type silicon photocathodes under illumination. Using the same catalyst, Smieja *et al*. observed a decreased catalytic current density on hydrogen-terminated p-Si which they improved by styrene functionalization of the electrode surface, an improvement attributed to better charge transfer resulting from pi interactions between styrene and the catalyst bipyridine ligand.[21] On p-type photocathodes, surface accumulation of photogenerated minority carriers (electrons) can result in a charged electrode, similar to our n-type TiO_2 in accumulation. While the origin of the current limitation was not precisely identified in that study, their result suggests the possibility of repulsive effects in support of our observations, and their surface functionalization approach represents a different pathway to overcoming the limitation.

Conclusions

We have demonstrated for the first time the efficient reduction of carbon dioxide to carbon monoxide on protected Cu_2O photocathodes using a molecular catalyst. The device produced high photovoltages of 560 mV and a photocurrent density of 2.1 mA cm^{-2}, corresponding to the highest photocurrent observed towards CO_2 reduction on an oxide material. Protection of the Cu_2O photocathode by TiO_2 enabled stable and selective reduction of CO_2 over several hours, and we found that protic electrolyte additives were needed to overcome the unexpected charge transfer limitations on the protected photocathode surface. From these observations of charge transfer, we propose that the protic species modifies the catalytic pathway to avoid charged catalyst intermediates. The discovery of charge transfer limitations from the surface of TiO_2 to the rhenium-based molecular catalyst and its elimination by the use of protic additives is highly relevant to the field of photoelectrochemistry, where there is a general trend towards the use of protective overlayers. We therefore expect our findings to be broadly applicable in photoelectrochemical systems involving semiconductors and molecular catalysts.

Notes and References

[a] Laboratory of Photonics and Interfaces, Institute of Chemical Sciences and Engineering, École Polytechnique Fédérale de Lausanne, CH-1015 Lausanne, Switzerland. E-mail: michael.graetzel@epfl.ch

† Electronic Supplementary Information (ESI) available: Experimental details and additional figures. See DOI: 10.1039/c000000x/

Acknowledgements

The authors thank Siemens AG for financial support. M.G. and T.M. thank the European Research Council for financial support under the Advanced Research Grant (ARG 247404) "Mesolight." P.G. thanks the European Community's Seventh Framework Programme (FP7/2007-2013) ENERGY.2012.10.2.1; NANOMATCELL, grant agreement no. 308997. M.T.M. acknowledges financial support from the FP7 Future and Emerging Technologies (FET) collaborative project "PHOCS" (contract no. 309223). Thanks to Prof. Christos Comninellis and Prof. Hubert Girault for support and helpful comments and to Dr. Manuel Méndez for proofreading the manuscript. Also, we would like to thank Dr. Fabrizio Giordano for supplying crystalline anatase TiO_2 layers.

References

1. Intergovernmental Panel on Climate Change, Ed., in *Climate Change 2013 - The Physical Science Basis*, Cambridge University Press, Cambridge, 2014, pp. 1–30.
2. J. Olivier, G. Janssens-Maenhout, M. Muntean and J. Peters, *Trends in global CO2 emissions: 2013 Report*, PBL Netherlands Environmental Assessment Agency Institute for Environment and Sustainability (IES) of the European Commission's Joint Research Centre (JRC), The Hague, 2013.
3. M. E. Boot-Handford, J. C. Abanades, E. J. Anthony, M. J. Blunt, S. Brandani, N. M. Dowell, J. R. Fernández, M.-C. Ferrari, R. Gross, J. P. Hallett, R. S. Haszeldine, P. Heptonstall, A. Lyngfelt, Z. Makuch, E. Mangano, R. T. J. Porter, M. Pourkashanian, G. T. Rochelle, N. Shah, J. G. Yao and P. S. Fennell, *Energy Environ. Sci.*, 2013, **7**, 130–189.
4. N. S. Lewis and G. Crabtree, *Basic Research Needs for Solar Energy Utilization: report of the Basic Energy Sciences Workshop on Solar Energy Utilization, April 18-21, 2005*, US Department of Energy, Office of Basic Energy Science, Washington, DC, 2005.
5. K. S. Joya, Y. F. Joya, K. Ocakoglu and R. van de Krol, *Angew. Chem. Int. Ed.*, 2013, **52**, 10426–10437.
6. Y. Tachibana, L. Vayssieres and J. R. Durrant, *Nat. Photonics*, 2012, **6**, 511–518.
7. D. G. Nocera, *Acc. Chem. Res.*, 2012, **45**, 767–776.
8. B. Kumar, M. Llorente, J. Froehlich, T. Dang, A. Sathrum and C. P. Kubiak, *Annu. Rev. Phys. Chem.*, 2012, **63**, 541–569.
9. K. Sivula, F. Le Formal and M. Grätzel, *ChemSusChem*, 2011, **4**, 432–449.
10. A. Paracchino, V. Laporte, K. Sivula, M. Grätzel and E. Thimsen, *Nat. Mater.*, 2011, **10**, 456–461.
11. S. D. Tilley, M. Schreier, J. Azevedo, M. Stefik and M. Graetzel, *Adv. Funct. Mater.*, 2014, **24**, 303–311.

12. J. Azevedo, L. Steier, P. Dias, M. Stefik, C. T. Sousa, J. P. Araújo, A. Mendes, M. Graetzel and S. D. Tilley, *Energy Environ. Sci.*, 2014, DOI: 10.1039/C4EE02160F.
13. A. Paracchino, N. Mathews, T. Hisatomi, M. Stefik, S. D. Tilley and M. Grätzel, *Energy Environ. Sci.*, 2012, **5**, 8673–8681.
14. B. Seger, D. S. Tilley, T. Pedersen, P. C. K. Vesborg, O. Hansen, M. Grätzel and I. Chorkendorff, *RSC Adv.*, 2013, **3**, 25902–25907.
15. B. Seger, S. D. Tilley, T. Pedersen, P. C. K. Vesborg, O. Hansen, M. Grätzel and I. Chorkendorff, *J. Mater. Chem. A*, 2013, **1**, 15089–15094.
16. B. Seger, I. E. Castelli, P. C. K. Vesborg, K. W. Jacobsen, O. Hansen and I. Chorkendorff, *Energy Environ. Sci.*, 2014, **7**, 2397.
17. B. Seger, T. Pedersen, A. B. Laursen, P. C. K. Vesborg, O. Hansen and I. Chorkendorff, *J. Am. Chem. Soc.*, 2013, **135**, 1057–1064.
18. S. Hu, M. R. Shaner, J. A. Beardslee, M. Lichterman, B. S. Brunschwig and N. S. Lewis, *Science*, 2014, **344**, 1005–1009.
19. M. F. Lichterman, A. I. Carim, M. T. McDowell, S. Hu, H. B. Gray, B. S. Brunschwig and N. S. Lewis, *Energy Environ. Sci.*, 2014, **7**, 3334–3337.
20. R. Liu, Z. Zheng, J. Spurgeon and X. Yang, *Energy Environ. Sci.*, 2014, **7**, 2504–2517.
21. J. M. Smieja, E. E. Benson, B. Kumar, K. A. Grice, C. S. Seu, A. J. M. Miller, J. M. Mayer and C. P. Kubiak, *Proc. Natl. Acad. Sci.*, 2012, **109**, 15646–15650.
22. B. Kumar, J. M. Smieja and C. P. Kubiak, *J. Phys. Chem. C*, 2010, **114**, 14220–14223.
23. E. E. Barton, D. M. Rampulla and A. B. Bocarsly, *J. Am. Chem. Soc.*, 2008, **130**, 6342–6344.
24. R. Liu, C. Stephani, J. J. Han, K. L. Tan and D. Wang, *Angew. Chem. Int. Ed.*, 2013, **52**, 4225–4228.
25. J. M. Smieja and C. P. Kubiak, *Inorg. Chem.*, 2010, **49**, 9283–9289.
26. C. Costentin, S. Drouet, M. Robert and J.-M. Savéant, *Science*, 2012, **338**, 90–94.
27. D. C. Grills, Y. Matsubara, Y. Kuwahara, S. R. Golisz, D. A. Kurtz and B. A. Mello, *J. Phys. Chem. Lett.*, 2014, **5**, 2033–2038.
28. J. A. Keith, K. A. Grice, C. P. Kubiak and E. A. Carter, *J. Am. Chem. Soc.*, 2013, **135**, 15823–15829.
29. M. X. Tan, P. E. Laibinis, S. T. Nguyen, J. M. Kesselman, C. E. Stanton and N. S. Lewis, in *Progress in Inorganic Chemistry*, ed. K. D. Karlin, John Wiley & Sons, Inc., 1994, pp. 21–144.
30. S. N. Frank and A. J. Bard, *J. Am. Chem. Soc.*, 1975, **97**, 7427–7433.
31. A. J. Nozik and R. Memming, *J. Phys. Chem.*, 1996, **100**, 13061–13078.
32. S. Y. Lam, C. Louis and R. L. Benoit, *J. Am. Chem. Soc.*, 1976, **98**, 1156–1160.
33. K. A. Grice and C. P. Kubiak, in *Advances in Inorganic Chemistry*, ed. Michele Aresta and Rudi van Eldik, Academic Press, 2014, vol. Volume 66, pp. 163–188.
34. M. D. Sampson, J. D. Froehlich, J. M. Smieja, E. E. Benson, I. D. Sharp and C. P. Kubiak, *Energy Environ. Sci.*, 2013, **6**, 3748–3755.